



Computational Modelling of SO₂ and H₂S gas interacting with small diameter Au-doped (5, 0) zig-zag single-walled carbon nanotubes

V. W. Elloh^{1,2*}, E. O. Boadu¹, D. F. Ofosuhene¹ and I. Arhin¹

¹Department of Biomedical Engineering, FHLAS, Koforidua Technical University, Ghana

²Department of Physics, University of Petroleum and Energy Studies (UPES), Dehradun, India

^{2*}Correspondence: vanw.elloh@ktu.edu.gh

Abstract

An ab initio density functional theory (DFT) is employed to explore the effect of adsorption of SO₂ and H₂S gases on gold-doped small diameter (5,0) zig-zag single-walled carbon nanotubes. Au-SWCNT nanostructures are extremely sensitive to the presence of both SO₂ and H₂S gases. Charge is transferred from the Au-SWCNT to the SO₂ upon the adsorption of the gas molecules onto the Au-SWCNT's surface. There is a decrease in the energy bandgap of the Au-SWCNT. As a consequence, the electrical conductivity of Au-SWCNTs/SO₂ is extremely enhanced. On the contrary, the adsorption of H₂S gas onto the surface of the gold-doped nanotube provokes charge transfer from H₂S to the Au-SWCNT. Another interesting observation is that the energy bandgap of Au-SWCNT increases upon the adsorption of the H₂S gas molecules onto the Au-SWCNT surface, thereby decreasing the electrical conductivity of the Au-SWCNT/H₂S nanostructure.

Keywords: DFT; GGA-PBE; LDA; small diameter; computational modelling; (5, 0) SWCNTs; Au-doped

Citation: Elloh, V. W., Boadu, E. O., Ofosuhene, D. F. and Arhin, I. (2021). **Computational Modelling of SO₂ and H₂S gas interacting with small diameter Au-doped (5, 0) zig-zag single-walled carbon nanotubes.** International Journal of Technology and Management Research (IJTMR), Vol. 6 (2): Pp.87-95.

Received: March 20, 2021

Accepted: September 1, 2021

1.0 Introduction

One of the most cherished applications of carbon nanotubes discovered by Iijima in 1991 [Iijima, 1991] is CNT-based gas sensors. CNT sensors exhibit a faster response, higher sensitivity, smaller size and lower working temperatures [Zhang *et al.*, 2000], CNT sensors can successfully detect a variety of gases [Kong *et al.*, 2000; Li *et al.*, 2003; Novak *et al.*, 2003; Chen and Wang, 2006; Wang *et al.*, 2007]. These characteristics are some of the merits of CNT sensors over the traditional gas sensors. Additionally, studies have shown that gold nanoparticles have a high sensitivity, good electrical conductivity and excellent catalytic activity [Daniel and Astruc, 2004; Zhang *et al.*, 2005; Tansil and Gao, 2006; Thaxton *et al.*, 2006]. To a very large extent, nowadays, gold is being used to modify and improve the intrinsic characteristics of CNTs.

Syed *et al.* [Mubeen *et al.*, 2009] have vividly shown in their studies that Au-nanoparticle-modified single-walled carbon nanotube (SWCNTs) sensors have a good sensitivity to H₂S at room temperature. Penza *et al.* [Penza *et al.*, 2007] have pointed out that Pt- and Au-functionalized CNTs are more sensitive by an order of magnitude for NH₃ and NO₂ detection and that the response time of the sensor was reduced. It was reported in Ref. [Zanolli *et al.*, 2011] that there was gigantic charge transfer in the process of adsorption of NO₂ and CO on Au-modified CNTs. The Fermi level, “E_F, of the nanotube was also noted to have altered accordingly.

In recent years, [Butler *et al.*, 2013] carbon nanomaterial, graphene due to its excellent properties of being highly sensitive to the detection of plethora of gas molecules, large sensing area per unit volume, low electronic temperature noise, fast response time and high chemical stability [Schedin *et al.*, 2007; He *et al.*, 2012] has become prominent in gas sensor applications. 2D nanomaterials have excellent surface-to-volume ratio, large accompanying charge transfer between gas molecules and associated substrates.

Gallium nitride (GaN) nanomaterials are also good candidates for gas sensors because they have outstanding electronic properties [Chitara *et al.*, 2010; Barth *et al.*, 2010; Pearton *et al.*, 2010; Abdulsattar *et al.*, 2016; Khan and Srivastava 2016; Cui *et al.*, 2017; Yong *et al.*, 2016; Baik *et al.*, 2017]. It has been shown theoretically in Ref. [Cui *et al.*, 2017] that Ga₁₂N₁₂ nanoclusters are potentially good NO, NO₂ and HCN gas sensors. In Ref. [Yong *et al.*, 2016], it has been demonstrated that cluster-assembled nanowires based on the Ga₁₂N₁₂ cluster can be an appropriate gas sensor for CO, NO and NO₂ detection.

Chemical sensors based on single-walled carbon nanotubes (SWCNTs) are the most efficient techniques for detecting gaseous molecules [Snow *et al.*, 2005]. Chemical sensors based on SWCNTs are for detecting contaminant and gaseous molecules, characterized” with a fast response time, high sensitivity and small size at room temperature [Jhi *et al.*, 2000]. In Refs. [Zhou *et al.*, 2010; Yoosefian *et al.*, 2014], adsorption of CH₄, CH₃OH, SO₂ and CO molecules on Pd-doped (5,5) SWCNTs (Pd/SWCNTs) have been explored. Due to its strong binding energy and large charge transfer effects, Pd/SWCNTs, exhibited high sensitivity to these molecules. Besides Pd nanoparticles, Pt nanoparticles were also used to functionalize multi-walled carbon nanotubes as excellent room-temperature hydrogen sensors [Star *et al.*, 2006; Kumar *et al.*, 2006; Kaniyoor *et al.*, 2009]. It has been shown in Refs. [Yeung *et al.*, 2008; Yeung *et al.*, 2007] that electronic structures of gas–Pt/CNTs complexes are powerfully affected by the presence of NO, NH₃, N₂, CO, C₂H₂, C₂H₄ and H₂ gases.

Adsorption of CH₄, CH₃OH, SO₂ and CO molecules on Pd-doped (5,5) SWCNTs (Pd/SWCNTs) have been explored [Zhou *et al.*, 2010; Yoosefian *et al.*, 2014]. The current work seeks to employ first-principles calculations procedures to explore the effects of adsorption of SO₂ and H₂S gases on gold-doped small diameter (5,0) zig-zag single-walled carbon nanotubes.

2.0 Methodology

In this work, “ab initio calculations within the density functional theory (DFT) method using the plane wave basis sets implemented in the Quantum Espresso code [Giannozzi *et al.*, 2017] has been employed. The generalized gradient approximation in the Perdew, Burke and Ernzerhof (PBE) form with van der Waals (vdW) correction, as proposed by Tkatchenko and Scheffler (TS method)” [Tkatchenko and Scheffler, 2009], was chosen to describe the exchange–correlation energy function. “Grimme van der Waals (vdW) dispersion correction is a necessary tool to account for the adverse effects of dispersion forces. We use the ultrasoft pseudopotentials [Rappe *et al.*, 1990]

in modelling the interactions between the ions and electrons with Perdew-Burke-Ernzerhof (PBE) exchange-correlation functional [Perdew *et al.*, 1996]. The Methfessel-Paxton smearing technique is used in the smearing of occupation numbers with Gaussian broadening of up to 0.001 Ry [Bjorkman and Granas, 2011].

We adopt the supercell model for (5,0) SWCNT where the nanotube is infinite and continuous. Our supercell consists of a semiconducting zigzag (5,0) SWCNT and molecular SO₂ and H₂S gases. A zigzag (5,0) SWCNT is chosen because of its semiconducting property and small diameter size in order to minimize the computational cost. A plane wave energy cutoff of 30 Ry is used and periodic boundary conditions are applied. The supercell is oriented along the x-axis and unit cell geometry with a vacuum space of 14 Å thick in both y- and z-directions are allowed to ensure negligible interactions between the tube and its periodic images with a supercell lattice parameter of 7.849 Å. The structure is optimized with the Broyden-Fletcher Goldfarb-Shanno (BFGS) method [Fletcher, 1987]. Next, we sample with a Γ -centred 5x1x1 Monkhorst-Pack scheme [Monkhorst and Pack, 1976] k-point grid. This is followed by fine 9x1x1 grids for a non-self-consistent field (NSCF) calculations to determine quantized energy levels and Fermi energy for band structure calculations in the Gamma-Z direction along the tube axis, charge density analysis, projected density of electronic states (DOS) and partial density of electronic states (PDOS).

3.0 Results and Discussions

3.1 Geometry Structure of the Nanostructure Models

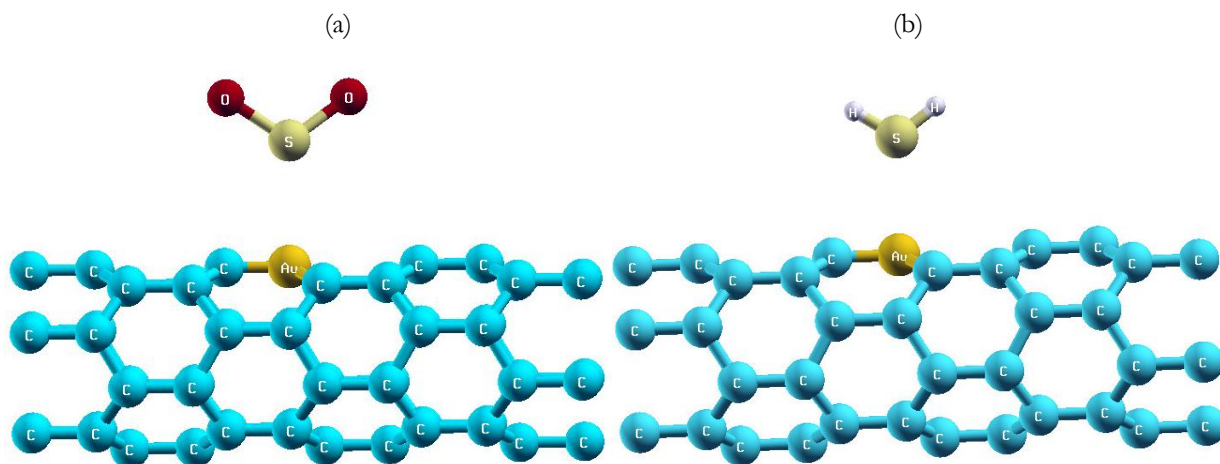


Figure 1. Optimized geometric structures of (a) Au-SWCNT/SO₂, (b) Au-SWCNT/H₂S nanostructures with a nanotube diameter of 3.917 Å with Au-SWCNT/SO₂ and Au-SWCNT/H₂S separations distance of \sim 2.691 Å and 2.524 Å respectively.

The structural geometry and stability of SO₂ and H₂S gases interacting with gold-doped small diameter (5,0) zig-zag single-walled carbon nanotubes as a composite model in a supercell structure has been studied. We have examined different structural geometries and stability of SO₂ and H₂S molecular gases interacting with Au-SWCNTs. The SO₂ and H₂S molecules have been aligned parallel to the Au-SWCNTs along with their side groups towards and/or away from the Au-SWCNTs. Other structural combinations and orientations notably with the SO₂ and H₂S molecules curved around the gold-doped nanotube and by flipping the SO₂ and H₂S molecules through 180° about their centres have been considered in order to determine the preferred orientations of the Au-SWCNT/SO₂ and Au-SWCNT/H₂S nanostructure geometries. It has been found that the SO₂ and H₂S molecules prefer to align with their side groups pointing away from the Au-SWCNTs. We have noted that the enthalpy of formations for these particular structural arrangements are lower than that of all other orientations examined. These are therefore energetically more stable and favorable. These orientations are therefore used for this study (Figure 1). The

molecular structures of Au-SWCNT/SO₂ and Au-SWCNT/H₂S composites shown in Figure 1 are similar to the stable orientation models reported in literature, [Xiaoxing *et al.*, 2014]. Figures 1(a & b) show the views of the optimized geometric” structures of Au-SWCNT/SO₂ and Au-SWCNT/H₂S nanostructure composites. The enthalpies of formation for the two configurations are low compare to similar structures in literature, therefore, energetically stable. Additionally, the negative formation energies imply the configurations (see Fig. 1) are thermodynamically favorable for studies. This closely agrees with the results obtained in Ref. [Yoosefian *et al.*, 2015].

The optimized structures give Au-SWCNT/SO₂ and “Au-SWCNT/H₂S interaction distances of $\sim 2.691 \text{ \AA}$ and 2.524 \AA respectively with a nanotube of diameter 3.917 \AA . The interlayer distances calculated are slightly shorter than the interlayer separations in graphite (ca. 3.35 \AA). The reason for the shorter distances of interactions in our nanostructures could be due to the presence of other functional groups on the Au-SWCNT/SO₂ and Au-SWCNT/H₂S nanostructure composites hence making them polar towards the nanotube during interaction.

Relative to the adsorption distances of $\sim 2.691 \text{ \AA}$ and 2.524 \AA , we calculated the adsorption energies, E_{ad} , for the Au-SWCNT/SO₂ and Au-SWCNT/H₂S nanostructure models in this case to be -1.271 and -1.349 respectively. The adsorption energies, E_{ad} , are determined from the relation:

$$E_{ad} = (E_{Au-SWCNT/SO_2} - E_{Au-SWCNT} - E_{SO_2}) \quad (1)$$

where $E_{Au-SWCNT/SO_2}$, $E_{Au-SWCNT}$, E_{SO_2} represent the total ground-state energy of the $E_{Au-SWCNT/SO_2}$ nanostructure, the total energy of $E_{Au-SWCNT}$, the total energy of E_{SO_2} respectively and similar procedures for Au-SWCNT/H₂S nanostructure. Quantum Espresso code reports the value of dispersion contribution to total energy for every step during the geometry optimization process. Accordingly, the dispersion contribution to adsorption energy is determined using Equation 1 above, by replacing the terms on the right-hand side with the dispersion contribution quantities for the converged geometry of each structure.

3.2 Electronic Properties

The electronic band structures at high-symmetry k-points for Au-SWCNT/SO₂ and Au-SWCNT/H₂S nanostructure models are shown in Figure 2. The calculated band gaps for the three nanostructures, Figures 2 (a, b & c), are 0.163 eV , 0.238 eV and 0.318 eV respectively.

Since GGA calculations tend to underestimate energy band-gaps of materials, there is a possibility that our currently calculated band-gap energies may not be exact in comparison to the experimental values. However, this difference may not be too significant but the origin could be attributed to the fact that, the exact form of the exchange correlation used is unknown. The band gaps occur due to mixed hybridization of valence states of O and Au with that of C atoms in the respective nanostructures.

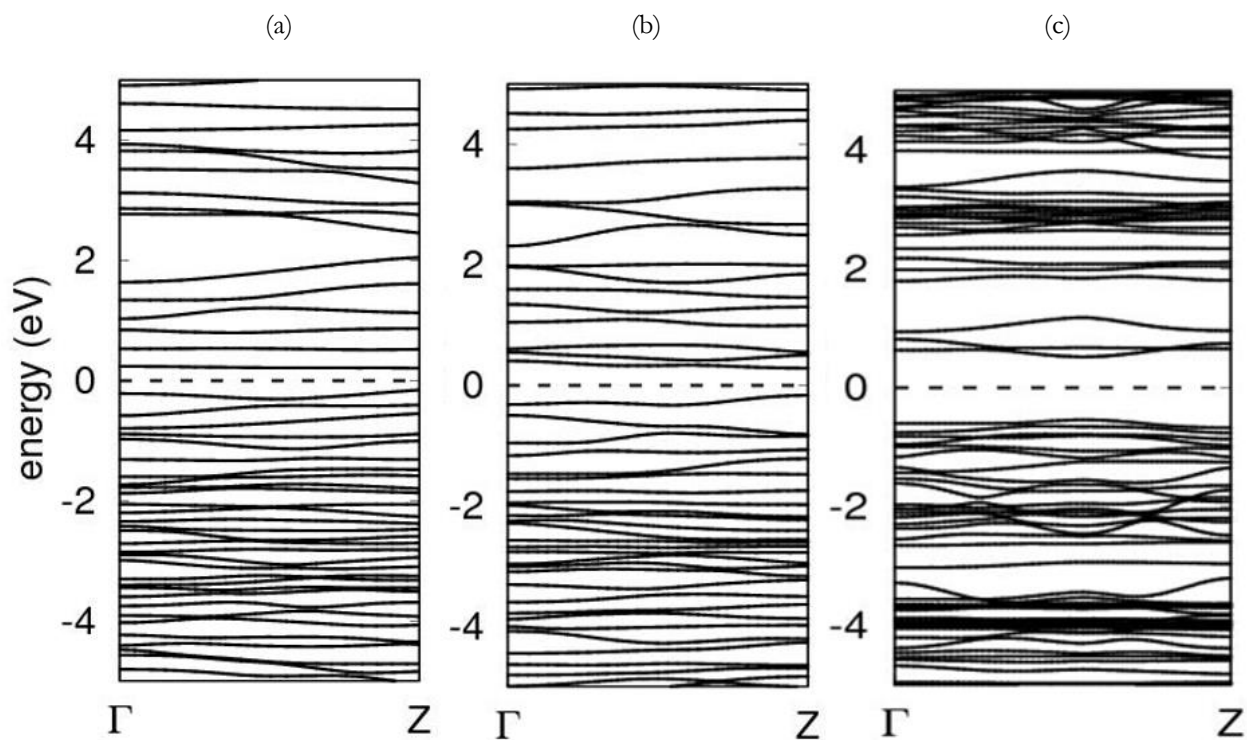


Figure 2. Calculated band structures at high-symmetry k -points of the gold-doped nanotube with fermi energy level set at zero for: (a) Au-SWCNT/SO₂, (b) Au-SWCNT, (c) Au-SWCNT/H₂S nanostructures respectively.

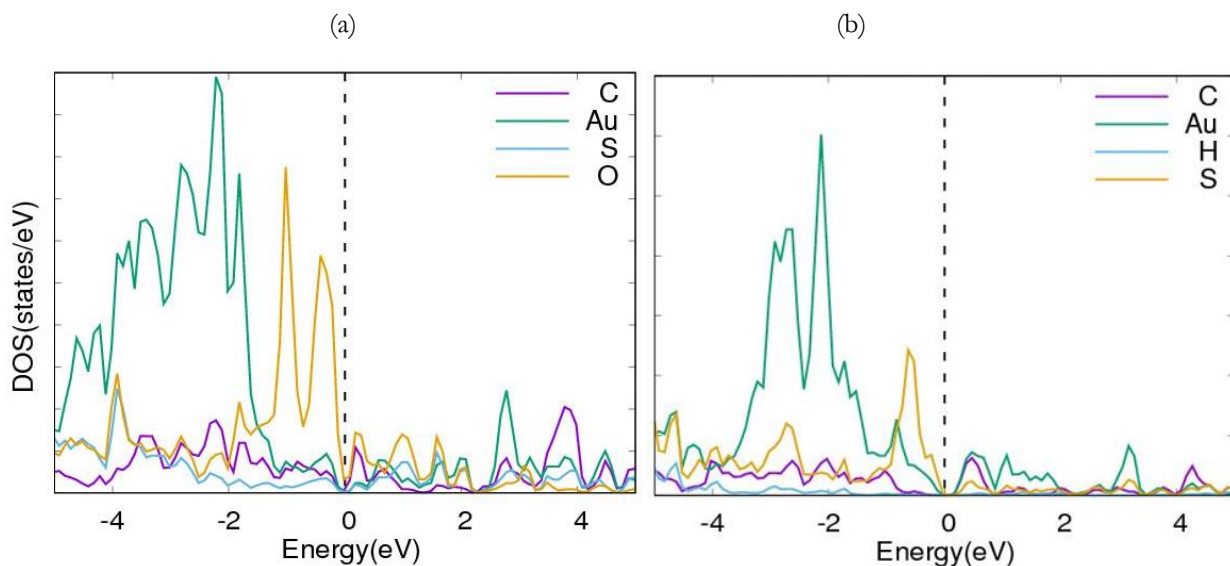


Figure 3. Projected electronic density of states (DOS) for the gold-doped nanotube with fermi energy level set at zero for: (a) Au-SWCNT/SO₂, (b) Au-SWCNT/H₂S nanostructures respectively.

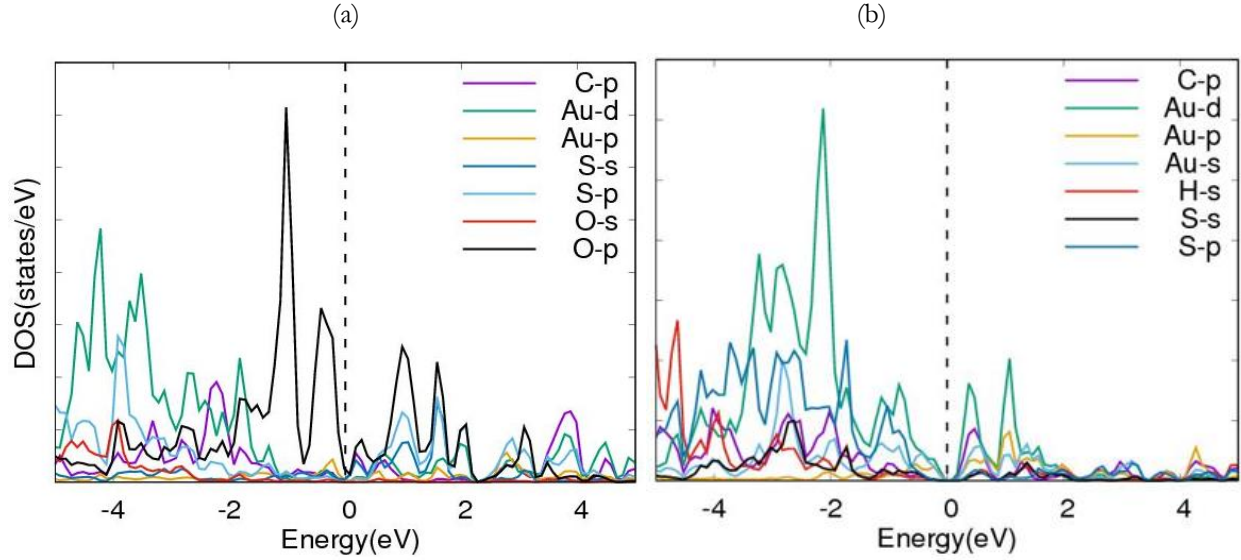


Figure 4. Partial electronic density of states (*p*-DOS) for the gold-doped nanotubes with fermi energy level set at zero for: (a) Au-SWCNT/SO₂, (b) Au-SWCNT/H₂S nanostructures.

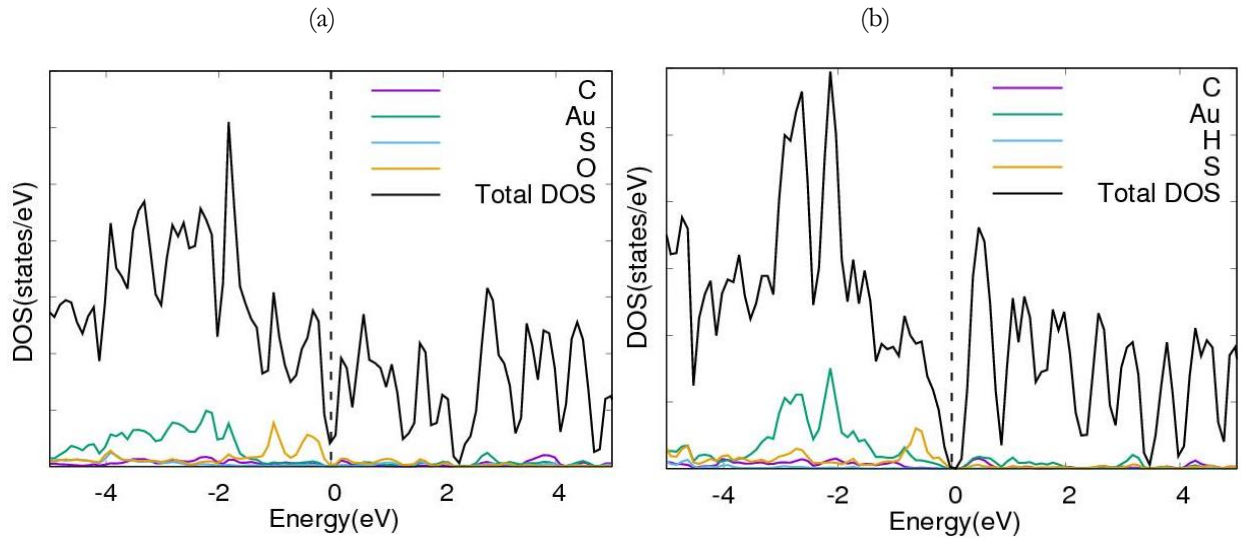


Figure 5. Total DOS (*t*-DOS) and projected electronic density of states (DOS) for: (a) Au-SWCNT/SO₂, (b) Au-SWCNT/H₂S nanostructures superimposed.

Upon further analysis of the electronic band structure plots, Figures 2(a, b & c), it is found out that these nanostructures are narrow and direct band gap materials with band gap values of 0.163, 0.238 and 0.318 eV, with the valance band and conduction band located at the high-symmetry k-points. This then makes them good candidates for photo physical applications because they are preferred materials for the fabrication of optoelectronic devices. These new materials have tunable band gaps and may find applications in various fields and are promising candidates to facilitate the development of band gap engineering for applications in infrared optoelectronics, nanoelectronics as well as gas sensors. By matching the band structures of (5,0) SWCNT and Au-SWCNTs with the new modelled nanostructures it is revealed that the new bands are formed as a result of the hybridization of the O-p and Au-d orbital states in the modelled nanostructures.

We further analyze the nature of interactions and origin of energy gaps in these nanostructures by way of plotting the projected electronic density of states (DOS), total DOS (t-DOS) and partial DOS (p-DOS) of the individual Au-SWCNT/SO₂ and Au-SWCNT/H₂S nanostructures in Figures 3, 4 and 5 respectively. For comparison, the Fermi energy, E_F, level was set as zero on the energy scale of the energy band-gap, E.g., between the occupied atomic orbitals and the empty atomic bands and same for the DOS, which are shown in Figures 3, 4 and 5. The total and partial electron density of states (t-DOS and p-DOS) plainly reveal that, the portion of DOS below -2 eV is due to Au and C atoms even though larger proportion of the contributions is coming from Au atoms only (Figure 4a). The central portion which is above -2 eV is due to the contributions from O and Au atoms in addition to the contribution of C atoms (Figure 4a). In Figure 4b, the portion of DOS below -2 eV is due to Au, C and S atoms even though larger proportion of the contributions is coming from Au atoms only. The central portion which is above -2 eV is due to the contributions from Au atoms in addition to the contribution of S atoms. The Figures 3, 4 and 5 show only positive contributions to the total and partial density of states of electrons for the Au-SWCNT/SO₂ and Au-SWCNT/H₂S nanostructures.

Upon the visualization of the atomic orbitals, we note that the DOS near the energy gaps is essentially of p_z electronic character manifestations of the anti-bonding and bonding of O atoms hybridizing with those of p_z states of gold and carbon atoms, (Figure 4a). From the p-DOS shown in Figure 4a, it can be seen that, the p-orbitals of oxygen and also p-orbitals of gold are the dominant class of contributors to the valence bands and the conduction band includes p-orbitals of carbon. Hence, both top of fully filled bands and the bottom of unoccupied bands are influenced by p-orbital states of oxygen, gold and carbon atoms resulting in the non-covalent π -stacking in Au-SWCNT/SO₂ and Au-SWCNT/H₂S nanostructure stackings as seen in Figures 1(a & b). In Figure 4b, the d-orbitals of gold are the dominant class of contributors to both valence and conduction bands.

3.3 Löwdin Charge Transfer Analysis

Using Löwdin charge transfer method [Löwdin 1950; Löwdin 1970], we calculated the average charge lost by gold and carbon species to be 0.15e and 0.04e respectively as shown in Table 1. We computed the average charge gained by sulphur and oxygen atoms as 0.89e and 0.78e respectively also shown in the table. Next, we expressed the atoms involved in Au-SWCNT in the form Au_xC_y and that of the SO₂ as S_mO_n , where x, y, m and n are the number of atoms involved. We then multiplied the average charge lost by C in Au-SWCNT by y , added it to the average charge lost by Au multiplied by x , this then gave us the total charge lost by Au-SWCNT. We multiplied the average charge gained by S by m , added it to the charge gained by O multiplied by n . The algebraic sum of these two processes gave us the charge transferred from the Au-SWCNT to the SO₂. This analysis confirms that there is charge distribution involving gold, carbon, sulphur and oxygen atoms. In effect, there is charge transfer of 2.45e from Au-SWCNT to the SO₂. The values presented in Table 1 are the average values for the specific sites. The spilling parameter of approximately 0.086e is not assigned to any atom by Löwdin method. Following similar procedures, there is a charge transfer of about 2.47e from H₂S to the Au-SWCNT nanostructure as depicted in Table 2.

Table 1: Calculation of charge transfer for Au-SWCNT/SO₂ using Löwdin charge analysis.

Neutral Atom	Valence Electron (e)	Average charge (e)	Average Charge lost/gain (e) ^{''}
S	6.00	6.89	0.89 ⁺
O	6.00	6.78	0.78 ⁺
Au	1.00	0.85	0.15 ⁻
C	4.00	3.96	0.04 ⁻

Key: electron lost/gain = -/+

Table 2: Calculation of charge transfer for Au-SWCNT/H₂S using Löwdin charge analysis.

Neutral Atom	Valence Electron (e)	Average charge (e)	Average Charge lost/gain (e)
H	1.00	0.18	0.82 ⁻
S	6.00	5.17	0.83 ⁻
Au	1.00	1.65	0.65 ⁺
C	4.00	4.03	0.03 ⁺

Key: electron lost/gain = -/+

4.0 Conclusion

In conclusion, using first-principles calculations based on density functional theory, the effect of adsorption of gas molecules, SO₂ and H₂S on the “Au-SWCNT nanostructure surface have been explored. We have obtained the adsorption geometries, adsorption energies, charge transfer and electronic properties of each molecule on the Au-SWCNT nanostructure. It is found that SO₂ and H₂S gas molecules are chemisorbed on the Au-SWCNT nanostructures. As a result of the adsorption of SO₂ and H₂S molecules, the electronic properties of the Au-SWCNT nanostructures exhibit remarkable phenomenal transformations, especially regarding their electrical conductivities. For the appreciable adsorption energies, the change in the electrical conductivity and the evident charge transfer, Au-SWCNT nanostructures can be used as a good sensor to detect” the presence of both SO₂ and H₂S in the environment. The bandgap of Au-SWCNT nanostructures can be deliberately tuned leading to promising bandgap engineering candidate for applications in infrared optoelectronics, nanoelectronics as well as gas sensors.

References

- A. M. Rappe, K. M. Rabe, E. Kaxiras, J. D. Joannopoulos, (1990). Optimized pseudopotentials, *Phys. Rev. B* 41-1227
- A. Kaniyoor, R.I. Jafri, T. Arockiadoss, S. Ramaprabhu, (2009). Nanostructured Pt decorated graphene and multi walled carbon nanotube-based room temperature hydrogen gas sensor, *Nanoscale* 1-382.
- A. Star, V. Joshi, S. Skarupo, D. Thomas, J.-C.P. Gabriel, (2006). Gas sensor array based on metal-decorated carbon nanotubes, *J. Phys. Chem. B* 110-21014.
- A. Tkatchenko and M. Scheffler, (2009). *Phys. Rev. Lett.* 102-073005.
- B. Chitara, D. J. Late, S. B. Krupanidhi and C. N. R. Rao, (2010). *Solid State Commun.*, 150-2053.
- C.S. Yeung, L.V. Liu, Y.A. Wang, (2007). Novel nanotube-coordinated platinum complexes, *J. Comput. Theor. Nanosci.* 4-1108
- C.S. Yeung, L.V. Liu, Y.A. Wang, (2008). Adsorption of small gas molecules onto Pt-doped single-walled carbon nanotubes, *J. Phys. Chem. C* 112-7401.
- Chen, C. and Wang X, (2006). Adsorption of Ni (II) from aqueous solution using oxidized multiwall carbon nanotubes *Ind. Eng. Chem. Res.* 45-9144.
- Daniel, M. C. and Astruc, D. (2004). Gold nanoparticles: assembly, supramolecular chemistry, quantum-size-related properties, and applications toward biology, catalysis, and nanotechnology *Chem. Rev.* 104-293
- E. Snow, F. Perkins, E. Houser, S. Badescu, T. Reinecke, (2005). Chemical detection with a single-walled carbon nanotube capacitor, *Science* 307-1942.
- F. Schedin, A. K. Geim, S. V. Morozov, E. W. Hill, P. Blake, (2007). *Nat. Mater.*, 6-652.
- H. Cui, Y. Yong, H. Jiang, L. Yang, S. Wang, G. Zhang, M. Guo and X. Li, (2017). *Mater. Res. Express*, 4-015009.
- H. J. Monkhorst, J. D. Pack, (1976). *Phys Rev B* 13-5188 – 5192.
- Iijima, S. (1991). Helical microtubules of graphitic carbon. *Nature* 354, 56.
- J. Perdew, K. Burke, M. Ernzerhof, (1996). Generalized gradient approximation made simple, *Phys. Rev. Lett.* 77 3865–3868, *Phys. Rev. Lett.* 77.3865.

- K. H. Baik, J. Kim and S. Jang, (2017). *Sens. Actuators B* 238-462.
- Kong, J. et al., (2000). Nanotube molecular wires as chemical sensors *Science* 287-622
- Li, J. et al., (2003). Carbon nanotube sensors for gas and organic vapor detection *Nano Lett.* 3-929.
- M. A. Abdulsattar, (2016). *Superlattices Microstruct.*, 93-163.
- M. S. Khan and A. Srivastava, J. (2016). *Electroanal. Chem.*, 775-243.
- M. Yoosefian, Z. Barzgari, J. Yoosefian, (2014). Ab initio study of Pd-decorated singlewalled carbon nanotube with C-vacancy as CO sensor, *Struct. Chem.* 25-9.
- M.K. Kumar, S. Ramaprabhu, (2006). Nanostructured Pt functionlized multiwalled carbon nanotube based hydrogen sensor, *J. Phys. Chem. B* 110-11291.
- Mehdi Yoosefian, Mansour Zahedi, Adeleh Mola, Samira Naserian, (2015). *Applied Surface Science* 349-864.
- Mubeen, S. et al., (2009). Sensitive detection of H₂S using gold nanoparticle decorated single-walled carbon nanotubes *Anal. Chem.* 82-250.
- Novak, J. P. et al., (2003). Nerve agent detection using networks of single-walled carbon nanotubes *Appl. Phys. Lett.* 83-4026
- P. Giannozzi, O. Andreussi, T. Brumme, O. Bunau, M. Buongiorno Nardelli, M. Calandra, R. Car, C. Cavazzoni, D. Ceresoli, M. Cococcioni, N. Colonna, I. Carnimeo, A. Dal Corso, S. De Gironcoli, P. Delugas, R.A. Distasio, A. Ferretti, A. Floris, G. Fratesi, G. Fugallo, R. Gebauer, U. Gerstmann, F. Giustino, T. Gorni, J. Jia, M. Kawamura, H.Y. Ko, A. Kokalj, E. Kucukbenli, M. Lazzeri, M. Marsili, N. Marzari, F. Mauri, N.L. Nguyen, H.V. Nguyen, A. Otero-De-La-Roza, L. Paulatto, S. Ponce, D. Rocca, R. Sabatini, B. Santra, M. Schlipf, A.P. Seitsonen, A. Smogunov, I. Timrov, T. Thonhauser, P. Umari, N. Vast, X. Wu, S. Baroni, (2017). Advanced capabilities for materials modelling with Quantum ESPRESSO, *J. Phys. Condens. Matter.* 29.
- P. O. Löwdin, (1970). *Adv. Quantum Chem.* 5-185.
- P. O. Löwdin, J. (1950). *Chem. Phys.* 18-365.
- Penza, M. et al., (2007). Enhancement of sensitivity in gas chemiresistors based on carbon nanotube surface functionalized with noble metal (Au, Pt) nanoclusters *Appl. Phys. Lett.* 90, 173123.
- Q. He, S. Wu, Z. Yina and H. Zhang, (2012). *Chem. Sci.*, 3-1764
- R. Fletcher, (1987). *Practical Methods of Optimization*, New York, Wiley.
- S. Barth, F. Hernandez-Ramirez, J. D. Holmes and A. Romano-Rodriguez, (2010). *Prog. Mater. Sci.*, 55-563
- S. H. Jhi, S.G. Louie, M.L. Cohen, (2000). Electronic properties of oxidized carbon nanotubes, *Phys. Rev. Lett.* 85-1710.
- S. J. Pearton, F. Renb, Y. Wang, B. H. Chu, K. H. Chen, C. Y. Chang, W. Lim, J. Lin and D. P. Norton, (2010). *Prog. Mater. Sci.*, 55-1.
- S. Z. Butler, S. M. Hollen, L. Cao, Y. Cui, J. A. Gupta, (2013). *ACS Nano*, 7-2898.
- Tansil N C and Gao Z Nanoparticles in biomolecular detection *Nano Today* 1 (2006) 28
- Thaxton, C. S., Georganopoulou, D. G. and Mirkin, C. A. (2006). Gold nanoparticle probes for the detection of nucleic acid targets *Clin. Chim. Acta* 363-120.
- Torbjorn Bjorkman, Oscar Granas, (2011). Adaptive Smearing for Brillouin Zone Integration, *Int. Jour. of Quan. Chem.* 111 (5)-1025.
- Wang, R. X. et al., (2007). A novel aluminum-doped carbon nanotubes sensor for carbon monoxide *J. Mol. Struct. Theochem.* 806-93.
- X. Zhou, W.Q. Tian, X.-L. Wang, Adsorption sensitivity of Pd-doped SWCNTs to small gas molecules, *Sens. Actuators B: Chem.* 151-56.
- Xiaoxing Zhang, Ziqiang Dai, Qinchuan Chen and Ju Tang, (2014). *Physica. Scripta* 89-065803.
- Y. Yong, H. Jiang, X. Li, S. Lv and J. Cao, (2016). *Phys. Chem. Chem. Phys.*, 18-21431.
- Zanolli, Z. et al., (2011). Gas sensing with Au-decorated carbon nanotubes *ACS Nano* 5-4592.
- Zhang X X, Liu W T, Tang J and Xiao P, (2000). Study on PD detection in SF₆ using multi-wall carbon nanotube films sensor *IEEE Trans. Dielectr. Electr. Insul.* 17-833.
- Zhang, Z L et al., (2005). Electrochemical DNA sensing based on gold nanoparticle amplification *Anal. Bioanal. Chem.* 381-833